ChemComm

Reduction-responsive dithiomaleimide-based nanomedicine with high drug loading and FRET-indicated drug release†

Hua Wang,[a] Ming Xu,[a] Menghua Xiong[a] and Jianjun Cheng*[ab]

Dithiomaleimide-based camptothecin-containing nanoparticles are designed to have exceptionally high drug loading and are capable of reduction-responsive, FRET-indicated drug release.

Nanomedicine, making use of nanostructures with sizes of around 20–200 nm to deliver anticancer agents, has emerged as a promising modality for cancer treatment due to its capability of improving the pharmacological and pharmacokinetic profiles of anticancer agents.[1–4] Various types of nanostructural delivery vehicles have been developed, including lipid vesicles (mostly liposomes), micelles, nanoparticles (NPs) and drug–polymer conjugates. Among these nanomedicine platforms, lipid vesicles composed of a bilayer lipid structure feature in their superior stability and unique interactions with cell membrane, with multiple drug products being approved by FDA for clinical cancer treatment.[5–9] However, one key drawback of conventional lipid vesicles is their low drug loading (usually much less than 10%) due to the limited interior volume for drug encapsulation and formulation challenges.[10–13] Much effort has been devoted to improving the drug loading of lipid vesicles by changing the lipid materials and formulation methods. Often, marginally improved drug loading is accompanied by compromised vesicle structural stability.[14–17]

Apart from excellent stability and high drug loading, an ideal lipid vesicle should also be able to actively control the release of carried drugs. A large variety of lipid vesicles subject to controlled structural decomposition and drug release in response to various intracellular triggers have been reported.[18–27] The huge concentration gradient of glutathione (GSH) between the intracellular

($\sim$10 mM) and the extracellular environment ($\sim$0.002 mM) has presented a unique trigger for the design of reduction-responsive lipid vesicles.[28–33] However, the design of the GSH-responsive systems has been largely based on the incorporation of a disulfide bond. Despite its GSH-responsiveness, the disulfide bond can also be non-specifically cleaved at elevated temperature or by intense light irradiation, which could potentially lead to severe inter-molecular cross-linking with biological materials, such as proteins that have multiple disulfide bonds.[34–40] An interesting chemistry was reported recently involving the rapid, clean reaction of 2,3-dibromo-maleimide and thiols, which gives dithiomaleimide in quantitative yields.[41–44] The maleimide thioether bonds in the resulting dithio-maleimide conjugate could be substituted by excess thiols,[45,46] suggesting its potential for being used as a GSH-responsive moiety. Compared to the disulfide bond, the maleimide thioether bond has much better thermal- and photo-stability. Besides its reactivity towards thiols, dithiomaleimides were also reported to show a strong green fluorescence,[47,48] a property that can potentially be taken advantage of for designing functional drug delivery vehicles.

Here, we report a multifunctional dithiomaleimide-based drug delivery nanomedicine with very high drug loading, excellent stability, GSH responsiveness, and drug release self-reporting capability. In our design, camptothecin (CPT)-thiols as the hydro-phobic moiety were conjugated to *N*-propargyl-2,3-dibromo-maleimide, followed by conjugation of poly(ethylene glycol) (PEG) *via* click chemistry to yield an AB$_2$-type amphiphilic structure ((CPT)$_2$-Mal-PEG, Schemes 1 and 2), resembling the building block structure of liposomes with one hydrophilic head group and two hydrophobic hydrocarbon tails. (CPT)$_2$-Mal-PEG NPs with drug loading as high as $\sim$60% can be easily prepared *via* the diffusion method. Interestingly, when excited at 370 nm, (CPT)$_2$-Mal-PEG NPs showed a significant emission peak at 550 nm (dithiomaleimide emission wavelength) instead of at 438 nm (CPT emission wavelength), indicating the existence of the Förster resonance energy transfer (FRET) phenomenon between CPT and maleimide thioether bonds. In the presence of GSH, the maleimide thioether bonds could be rapidly cleaved, followed by

[a] *Department of Materials Science and Engineering, University of Illinois at Urbana–Champaign, 1304 West Green Street, Urbana, IL, 61801, USA. E-mail: jianjunc@illinois.edu*

[b] *Department of Bioengineering, University of Illinois at Urbana–Champaign, 1304 West Green Street, Urbana, IL, 61801, USA*
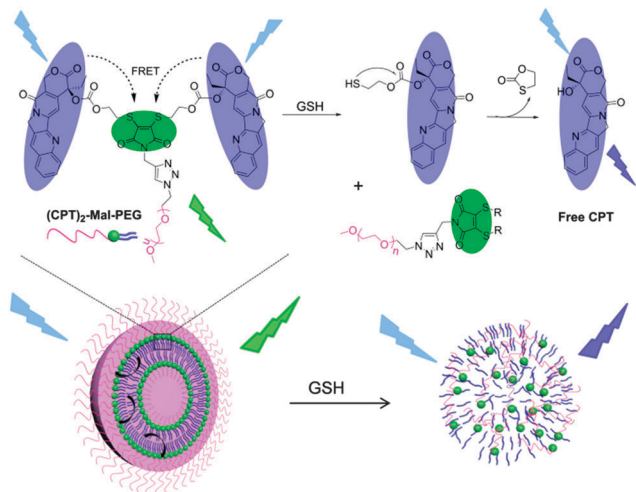
Scheme 1 Schematic illustration of GSH-mediated drug release and FRET inactivation of $(CPT)_2$-Mal-PEG NPs.
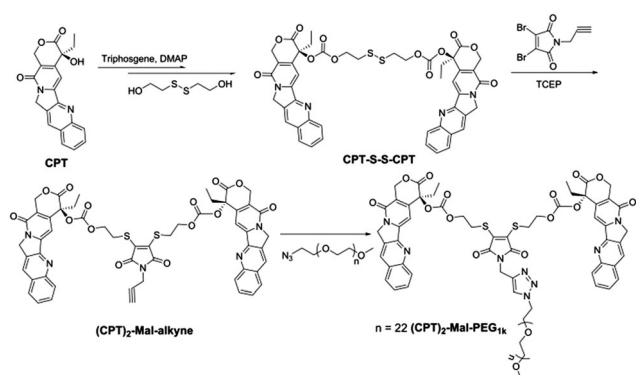
Scheme 2 Synthesis of reduction-responsive amphiphilic $(CPT)_2$-Mal-PEG.

Fig. 1 (a) Fluorescence spectra of $(CPT)_2$-Mal-PEG$_{1k}$ in methanol treated with 5 mM GSH for 0, 15, and 30 min, respectively. Excitation wavelength was set at 370 nm. Inset: pictures of $(CPT)_2$-Mal-PEG$_{1k}$ in methanol under UV irradiation (365 nm) before (left) and after (right) GSH treatment. (b) Correlation of I_{438}/I_{550} to the percentage of released CPT from $(CPT)_2$-Mal-PEG$_{1k}$ in the presence of 5 mM GSH. DLS (c) and TEM (d) characterizations of $(CPT)_2$-Mal-PEG$_{1k}$ NPs. The scale bar represents 200 nm.

cyclization reactions to release CPT and cause disruption of the NP structure. A reduction of the FRET signal was observed along with the release of free CPT, which provided a non-invasive tool to follow drug release from the $(CPT)_2$-Mal-PEG NPs.

CPT-S-S-CPT with a disulfide linker was first synthesized through the activation of CPT with triphosgene and further reaction with 2-hydroxyethyl disulfide (Scheme 2). CPT-S-S-CPT was then conjugated to N-propargyl-2,3-dibromomaleimide in the presence of tris(2-carboxyethyl)phosphine (TCEP) to yield $(CPT)_2$-Mal-alkyne. $(CPT)_2$-Mal-PEG was synthesized *via* the Click reaction between $(CPT)_2$-Mal-alkyne and PEG-N$_3$. The overall yield of these three-step reactions was around 35%.

We next selected $(CPT)_2$-Mal-PEG$_{1k}$ to evaluate its GSH-responsiveness and fluorescence properties. $(CPT)_2$-Mal-PEG$_{1k}$ in methanol showed a strong green fluorescence instead of a typical blue fluorescence of CPT under UV irradiation (365 nm) (inset, Fig. 1a). Analysis of $(CPT)_2$-Mal-PEG$_{1k}$ using a fluorescence spectrometer also showed a significant emission peak at 550 nm instead of 438 nm (CPT maximum emission wavelength) at an excitation wavelength of 370 nm (Fig. 1a, black line), suggesting the existence of the FRET phenomenon between CPT and maleimide thioethers.

To confirm this, the fluorescence spectra of free CPT and various dithiomaleimides were collected and compared (Fig. S6 and Table S1, ESI†). The maximum excitation and emission wavelengths of CPT are 370 nm and 438 nm, respectively, as compared to the maximum excitation and emission wavelengths of dithiomaleimides at 420–450 nm and 520–560 nm, respectively (Table S1, ESI†). Given the facts that the emission wavelength of CPT is very close to the maximum excitation wavelength of dithiomaleimides and these two fluorescent moieties are only 5σ bonds away from each other (<1 nm), it is therefore not surprising to observe the FRET phenomenon (Scheme 1). We then studied whether treatment with an excessive amount of GSH would release CPT from $(CPT)_2$-Mal-PEG$_{1k}$ and how the FRET signal would change over time upon GSH treatment. The emission of $(CPT)_2$-Mal-PEG$_{1k}$ at 438 nm was found to increase significantly, accompanied by the decrease of the emission intensity at 550 nm after being treated with 5 mM GSH for 15 min. After 30 min treatment with GSH at the same concentration, the emission intensity at 438 nm further increased while the peak at 550 nm disappeared, indicating the complete degradation of $(CPT)_2$-Mal-PEG$_{1k}$ which was confirmed using HPLC analysis (Fig. S7, ESI†). A correlation between the intensity ratio (I_{438}/I_{550}) and the percentage of released CPT from $(CPT)_2$-Mal-PEG$_{1k}$ showed a quasi-linear relationship (R^2 = 0.993, Fig. 1b and Fig. S8, ESI†). These experiments demonstrated that $(CPT)_2$-Mal-PEG$_{1k}$ can release free CPT rapidly in the reductive environment and the release of CPT correlates well with the decrease of the FRET signal between CPT and maleimide thioethers.

After demonstrating reduction-responsiveness and the FRET properties of $(CPT)_2$-Mal-PEG$_{1k}$, we next prepared $(CPT)_2$-Mal-PEG$_{1k}$ NPs by adding nanopure water to a DMF solution of $(CPT)_2$-Mal-PEG$_{1k}$ (DMF/H$_2$O, 1/40, v/v). NP with an average hydrodynamic size of 151 nm and a polydispersity (PDI) of

0.154 was obtained (Fig. 1c). TEM analysis confirmed the formation of nanostructures with an average size of 140 nm (Fig. 1d). As the structure of $(CPT)_2$-Mal-PEG_{1k} is similar to that of (OEG)-DiCPT, which was reported to form a nanocapsule structure by Shen and coworkers,[49] $(CPT)_2$-Mal-PEG_{1k} NP likely has a similar vesicle-like structure.

We next studied the GSH-responsive drug release and fluorescence properties of the prepared $(CPT)_2$-Mal-PEG_{1k} NPs. As expected, a significant emission peak at 550 nm was observed when the NPs were excited at 370 nm, indicating the existence of FRET signal between CPT and maleimide thioethers in the nanostructure (Fig. 2a, black line). Although the analysis here was based on the overall FRET effect, it should be noted that intermolecular FRET may also exist because of the closely packed nanostructures. With the change of the concentration of $(CPT)_2$-Mal-PEG_{1k} NP, the I_{438}/I_{550} value remained largely unchanged, suggesting that the FRET properties of the NP was independent of its concentration (Fig. S9, ESI†). We then studied the degradation of $(CPT)_2$-Mal-PEG_{1k} NPs in the presence of GSH. Compared to GSH-mediated degradation of $(CPT)_2$-Mal-PEG_{1k}, it took a much longer time for GSH to completely degrade the maleimide thioether structure of the $(CPT)_2$-Mal-PEG_{1k} NPs, presumably because of the well-packed $(CPT)_2$-Mal-PEG_{1k} nanostructure. After the NPs were incubated with 5 mM GSH for 2 h, the emission peak at 550 nm was largely reduced while the emission at 438 nm increased significantly, which could be explained by the GSH-induced cleavage of maleimide thioether bonds, release of CPT,

and disruption of the presumed nanocapsule structure. After the NPs were treated with 5 mM GSH for 8 h, I_{438}/I_{550} reached a plateau, indicating the complete degradation of the maleimide thioether structure. To further demonstrate the disruption of nanostructures upon GSH treatment, we monitored the size and the count rate of NPs in PBS over time (Fig. 2b). In the absence of GSH, the change of size and count rate was negligible over 5 days (Fig. 2b and Fig. S10, ESI†), demonstrating the excellent stability of $(CPT)_2$-Mal-PEG_{1k} NPs. In the presence of 5 mM GSH, however, the size of NPs increased from 151 nm to 733 nm at 5 h, and further increased to ∼1300 nm at 8 h, presumably due to the aggregation of the released CPT (Fig. 2b and Fig. S11, ESI†). Decreased count rate of the NP solution also suggested the disruption of the nanostructure over GSH treatment (Fig. 2b).

We next studied CPT release kinetics from $(CPT)_2$-Mal-PEG_{1k} NPs in the presence or absence of GSH. In the absence of GSH, negligible CPT release was observed over 24 h. In comparison, over 59% and 95% of CPT were released from $(CPT)_2$-Mal-PEG_{1k} NPs after the NPs were treated with 1 mM GSH and 5 mM GSH, respectively for 24 h (Fig. 2c). The CPT release profile of $(CPT)_2$-Mal-PEG_{1k} NPs in the presence of 5 mM GSH determined by HPLC correlated well with FRET-indicated release kinetics in the first 5 h (Fig. S12, ESI†). Differently from the unchanged I_{438}/I_{550} value after 8 h, release of free CPT increased continuously, which probably resulted from the difference between cleavage of maleimide thioether structure and release of free CPT. Despite the complete cleavage of maleimide thioether bonds, CPT might be entrapped in the dialysis tube and slowly diffuse into the release medium.

To demonstrate the proliferation inhibition capability of $(CPT)_2$-Mal-PEG_{1k} NPs, we investigated the cytotoxicity of NPs against LS174T colon cancer cells via an MTT (3-(4,5-dimethyl-thiazol-2-yl)-2,5-diphenyltetrazolium bromide) colorimetric assay. LS174T cells were incubated with $(CPT)_2$-Mal-PEG_{1k} NPs or free CPT at various CPT concentrations for 48 h, and the cell viability results were shown in Fig. 2d. $(CPT)_2$-Mal-PEG_{1k} NPs and free CPT showed an IC_{50} value of 177 nM (CPT equivalent) and 78 nM, respectively. To further demonstrate the reduction-responsive cytotoxicity of $(CPT)_2$-Mal-PEG_{1k} NPs, we investigated the viability of NP-treated LS174T cells with the addition of cellular GSH level regulators. GSH-OEt has been widely used to increase the GSH level via its hydrolysis after entering cells.[50–53] Prior to treatment with NPs, cells were pretreated with GSH-OEt for 4 h. As shown in Fig. 2d, GSH-OEt significantly decreased the IC_{50} value of $(CPT)_2$-Mal-PEG_{1k} NPs from 177 nM (CPT equivalent) to 108 nM (CPT equivalent). In comparison, free CPT showed a negligible change in IC_{50} with GSH-OEt pretreatment. This comparison well demonstrated the reduction-responsive cytotoxicity of $(CPT)_2$-Mal-PEG_{1k} NPs.

In conclusion, we have developed a multifunctional dithiomaleimide-based CPT-containing NP with very high drug loading (up to 60%). $(CPT)_2$-Mal-PEG_{1k} NPs showed great stability under physiological conditions while they underwent rapid disruption in the presence of GSH. Release of CPT from $(CPT)_2$-Mal-PEG_{1k} NPs in the presence of GSH was accompanied by a reduction of the
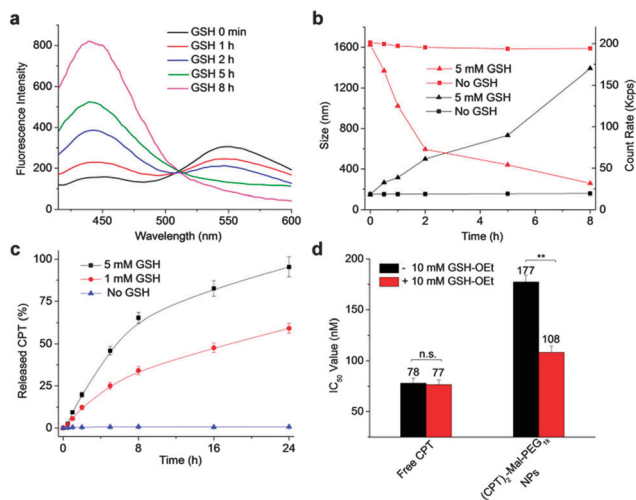
Fig. 2 (a) Fluorescence spectra of $(CPT)_2$-Mal-PEG_{1k} NPs in PBS (pH 7.4) after treated with 5 mM GSH for 0 min, 1 h, 2 h, 5 h, and 8 h, respectively. Excitation wavelength was set at 370 nm. (b) Changes of the size (black line) and the count rate (red line) of $(CPT)_2$-Mal-PEG_{1k} NPs over time in the presence (▲) or absence (■) of 5 mM GSH. (c) CPT release profiles of $(CPT)_2$-Mal-PEG_{1k} NPs in the presence of 0 mM, 1mM, and 5 mM GSH, respectively. (d) IC_{50} values of free CPT and $(CPT)_2$-Mal-PEG_{1k} NPs against LS174T colon cancer cells with or without GSH-OEt pretreatment. Data were presented as average ± standard deviation, n = 3. Statistical significance analysis was assessed by two-sample unpaired student's t-test; $0.01 < p \leq 0.05$ and $p \leq 0.01$ were considered statistically significant and highly significant and were denoted as "*" and "**" respectively.

View Article Online

Communication   ChemComm

FRET signal between CPT and maleimide thioethers, suggesting the drug-release self-reporting properties of $(CPT)_2$-Mal-PEG_{1k} NPs. *In vitro* anticancer efficacy study demonstrated the GSH-responsive cancer inhibitory effect of $(CPT)_2$-Mal-PEG_{1k} NPs. Further studies of $(CPT)_2$-Mal-PEG_{1k} NP, such as *in vivo* efficacy and structural analysis, are underway.

Notes and references

1 S. M. Moghimi, A. C. Hunter and J. C. Murray, *FASEB J.*, 2005, **19**, 311–330.
2 V. Wagner, A. Dullaart, A.-K. Bock and A. Zweck, *Nat. Biotechnol.*, 2006, **24**, 1211–1218.
3 O. C. Farokhzad and R. Langer, *Adv. Drug Delivery Rev.*, 2006, **58**, 1456–1459.
4 K. Riehemann, S. W. Schneider, T. A. Luger, B. Godin, M. Ferrari and H. Fuchs, *Angew. Chem., Int. Ed.*, 2009, **48**, 872–897.
5 J. Weinstein, E. Ralston, L. Leserman, R. Klausner, P. Dragsten, P. Henkart and R. Blumenthal, *Liposome Technol.*, 1984, **3**, 183–204.
6 M. Winterhalter and D. Lasic, *Chem. Phys. Lipids*, 1993, **64**, 35–43.
7 A. Gabizon, M. Chemla, D. Tzemach, A. Horowitz and D. Goren, *J. Drug Targeting*, 1996, **3**, 391–398.
8 Y. C. Barenholz, *J. Controlled Release*, 2012, **160**, 117–134.
9 A. Meyerhoff, *Clin. Infect. Dis.*, 1999, **28**, 42–48.
10 I. V. Zhigaltsev, N. Maurer, Q.-F. Akhong, R. Leone, E. Leng, J. Wang, S. C. Semple and P. R. Cullis, *J. Controlled Release*, 2005, **104**, 103–111.
11 A. Gabizon, H. Shmeeda, A. T. Horowitz and S. Zalipsky, *Adv. Drug Delivery Rev.*, 2004, **56**, 1177–1192.
12 S. Sofou and G. Sgouros, *Expert Opin. Drug Delivery*, 2008, **5**, 189–204.
13 N. Weiner, F. Martin and M. Riaz, *Drug Dev. Ind. Pharm.*, 1989, **15**, 1523–1554.
14 A. Mohammed, N. Weston, A. Coombes, M. Fitzgerald and Y. Perrie, *Int. J. Pharm.*, 2004, **285**, 23–34.
15 N. Dos Santos, K. A. Cox, C. A. McKenzie, F. van Baarda, R. C. Gallagher, G. Karlsson, K. Edwards, L. D. Mayer, C. Allen and M. B. Bally, *Biochim. Biophys. Acta, Biomembr.*, 2004, **1661**, 47–60.
16 D. Zucker, D. Marcus, Y. Barenholz and A. Goldblum, *J. Controlled Release*, 2009, **139**, 73–80.
17 M. Johnsson, N. Bergstrand and K. Edwards, *J. Liposome Res.*, 1999, **9**, 53–79.
18 T. L. Andresen, S. S. Jensen and K. Jørgensen, *Prog. Lipid Res.*, 2005, **44**, 68–97.
19 F. Ahmed, R. I. Pakunlu, A. Brannan, F. Bates, T. Minko and D. E. Discher, *J. Controlled Release*, 2006, **116**, 150–158.
20 J.-C. Leroux, E. Allémann, F. De Jaeghere, E. Doelker and R. Gurny, *J. Controlled Release*, 1996, **39**, 339–350.
21 V. Torchilin, F. Zhou and L. Huang, *J. Liposome Res.*, 1993, **3**, 201–255.
22 J.-C. Leroux, E. Roux, D. Le Garrec, K. Hong and D. C. Drummond, *J. Controlled Release*, 2001, **72**, 71–84.
23 P. Meers, *Adv. Drug Delivery Rev.*, 2001, **53**, 265–272.
24 J. Hu, G. Zhang and S. Liu, *Chem. Soc. Rev.*, 2012, **41**, 5933–5949.
25 M.-H. Li and P. Keller, *Soft Matter*, 2009, **5**, 927–937.
26 L. Liu, W. Wang, X.-J. Ju, R. Xie and L.-Y. Chu, *Soft Matter*, 2010, **6**, 3759–3763.
27 W. Wu, Q. Zhang, J. Wang, M. Chen, S. Li, Z. Lin and J. Li, *Polym. Chem.*, 2014, **5**, 5668–5679.
28 R. Cheng, F. Feng, F. Meng, C. Deng, J. Feijen and Z. Zhong, *J. Controlled Release*, 2011, **152**, 2–12.
29 B. Khorsand, G. Lapointe, C. Brett and J. K. Oh, *Biomacromolecules*, 2013, **14**, 2103–2111.
30 F. Meng, W. E. Hennink and Z. Zhong, *Biomaterials*, 2009, **30**, 2180–2198.
31 H. Wang, L. Tang, C. Tu, Z. Song, Q. Yin, L. Yin, Z. Zhang and J. Cheng, *Biomacromolecules*, 2013, **14**, 3706–3712.
32 K. Wang, G.-F. Luo, Y. Liu, C. Li, S.-X. Cheng, R.-X. Zhuo and X.-Z. Zhang, *Polym. Chem.*, 2012, **3**, 1084–1090.
33 K. Tanaka, W. Ohashi, N. Kitamura and Y. Chujo, *Bull. Chem. Soc. Jpn.*, 2011, **84**, 612–616.
34 U. Jakob, W. Muse, M. Eser and J. C. Bardwell, *Cell*, 1999, **96**, 341–352.
35 C. Donnet, E. Arystarkhova and K. J. Sweadner, *J. Biol. Chem.*, 2001, **276**, 7357–7365.
36 C. S. Love, I. Ashworth, C. Brennan, V. Chechik and D. K. Smith, *Langmuir*, 2007, **23**, 5787–5794.
37 X. Z. Shu, Y. Liu, F. Palumbo and G. D. Prestwich, *Biomaterials*, 2003, **24**, 3825–3834.
38 S. Zhou, O. Mozziconacci, B. A. Kerwin and C. Schöneich, *Pharm. Res.*, 2013, **30**, 1291–1299.
39 J. Jiang, B. Qi, M. Lepage and Y. Zhao, *Macromolecules*, 2007, **40**, 790–792.
40 K. Peters and F. M. Richards, *Annu. Rev. Biochem.*, 1977, **46**, 523–551.
41 M. W. Jones, R. A. Strickland, F. F. Schumacher, S. Caddick, J. R. Baker, M. I. Gibson and D. M. Haddleton, *J. Am. Chem. Soc.*, 2012, **134**, 1847–1852.
42 M. E. Smith, F. F. Schumacher, C. P. Ryan, L. M. Tedaldi, D. Papaioannou, G. Waksman, S. Caddick and J. R. Baker, *J. Am. Chem. Soc.*, 2010, **132**, 1960–1965.
43 M. W. Jones, R. A. Strickland, F. F. Schumacher, S. Caddick, J. R. Baker, M. I. Gibson and D. M. Haddleton, *Chem. Commun.*, 2012, **48**, 4064–4066.
44 M. P. Robin, M. W. Jones, D. M. Haddleton and R. K. O'Reilly, *ACS Macro Lett.*, 2011, **1**, 222–226.
45 A. B. Mabire, M. P. Robin, H. Willcock, A. Pitto-Barry, N. Kirby and R. K. O'Reilly, *Chem. Commun.*, 2014, **50**, 11492–11495.
46 A. D. Baldwin and K. L. Kiick, *Bioconjugate Chem.*, 2011, **22**, 1946–1953.
47 M. P. Robin and R. K. O'Reilly, *Chem. Sci.*, 2014, **5**, 2717–2723.
48 M. P. Robin, P. Wilson, A. B. Mabire, J. K. Kiviaho, J. E. Raymond, D. M. Haddleton and R. K. O'Reilly, *J. Am. Chem. Soc.*, 2013, **135**, 2875–2878.
49 Y. Shen, E. Jin, B. Zhang, C. J. Murphy, M. Sui, J. Zhao, J. Wang, J. Tang, M. Fan, E. Van Kirk and W. J. Murdoch, *J. Am. Chem. Soc.*, 2010, **132**, 4259–4265.
50 R. Hong, G. Han, J. M. Fernández, B.-j. Kim, N. S. Forbes and V. M. Rotello, *J. Am. Chem. Soc.*, 2006, **128**, 1078–1079.
51 N. Morito, K. Yoh, K. Itoh, A. Hirayama, A. Koyama, M. Yamamoto and S. Takahashi, *Oncogene*, 2003, **22**, 9275–9281.
52 A. N. Koo, H. J. Lee, S. E. Kim, J. H. Chang, C. Park, J. H. Park and S. C. Lee, *Chem. Commun.*, 2008, 6570–6572.
53 Y. C. Wang, Y. Li, T. M. Sun, M. H. Xiong, J. Wu, Y. Y. Yang and J. Wang, *Macromol. Rapid Commun.*, 2010, **31**, 1201–1206.